

https://goldncloudpublications.com https://doi.org/10.47392/IRJAEM.2025.0428 e ISSN: 2584-2854 Volume: 03

Issue: 08 August 2025 Page No: 2723 - 2734

Tailoring Structure, Morphology, And Magnetic Behavior in Eu-Doped Bafeo₃ Perovskite Nanomaterials

Dipak Nath ^{1,2}, A. Robert Xavier ³

- ¹ Research Scholar, Department of Physics, St. Joseph University, Chumoukedima, 797103.Nagaland, India.
- ² Associate Professor, Department of Physics, Kohima Science College Jotsoma, Kohima, 797002, Nagaland, India.
- ³Professor, Department of Physics, St. Joseph University, Chumoukedima, 797103, Nagaland, India. Emails: dipaknath03081976@gmail.com^{1,2}, arobertxavier@gmail.com³

Abstract

This study examines the influence of Europium (Eu) doping on the structural, morphological, and magnetic properties of barium ferrate (BaFeO₃), a perovskite oxide with potential for use in advanced technologies. BaFeO₃ samples were synthesized via the solution combustion method, a simple, rapid, and energy-efficient technique that produces fine, uniform powders with high purity. X-ray diffraction (XRD) analysis confirmed the formation of a single-phase cubic spinel perovskite structure. As the Eu doping concentration increased (0%, 5%, and 9%), a gradual decrease in crystallinity was observed, suggesting lattice distortion without any phase change. Field Emission Scanning Electron Microscopy (FESEM) showed a reduction in particle size and noticeable changes in surface morphology at higher doping levels. Magnetic measurements carried out using a Vibrating Sample Magnetometer (VSM) revealed significant changes in magnetic behavior due to Eu doping, including variations in saturation magnetization and coercivity. These findings indicate that Eu doping is an effective approach to modify and improve the physical and magnetic characteristics of BaFeO₃, making it more suitable for future functional, magnetic, and electronic applications.

Keywords: Europium, Barium ferrate perovskite nanomaterials, Solution combustion synthesis, X-ray diffraction, Field emission scanning electron microscopy, Vibrating Sample Magnetometer.

1. Introduction

Barium ferrite oxide (BaFeO₃) has considerable attention as a promising perovskite oxide owing to its versatile magnetic, electronic, and photocatalytic properties. These multifunctional features render it suitable for a range of advanced including high-density applications, storage, gas sensing, catalysis, and notably, spintronic technologies. Spintronics, which utilizes both the charge and spin of electrons, demands materials with controllable magnetic ordering, high spin polarization, and structural robustness. One effective strategy to achieve such perovskite functionalities in oxides incorporation of rare-earth elements into the crystal lattice, which can induce notable alterations in the structural and magnetic characteristics of the host material (Alahmari & Fatima, 2024). In this regard,

europium (Eu) has been introduced as a dopant in BaFeO₃ due to its distinctive 4f⁶ electronic configuration, variable oxidation states, pronounced spin-orbit coupling. These attributes play a pivotal role in modulating spin interactions and magnetic ordering within the crystal framework. As a lanthanide element, europium is known for its metallic nature, high reactivity, characteristic red luminescence. Its ability to exist in both +2 and +3 valence states offer dynamic control over charge compensation and defect chemistry key parameters for tuning the electronic and magnetic behaviours essential for spintronic applications. BaFeO₃ usually adopts a distorted perovskite structure of the orthorhombic GdFeO₃type (ABO₃), where Ba²⁺ occupies the A-site and Fe⁴⁺ the B-site. Substituting Ba²⁺ with the slightly



e ISSN: 2584-2854 Volume: 03

Issue: 08 August 2025 Page No: 2723 - 2734

https://goldncloudpublications.com https://doi.org/10.47392/IRJAEM.2025.0428

smaller Eu³⁺ ion introduces local lattice distortion and internal strain due to ionic radius mismatch, influencing the Fe-O-Fe bond angles and thereby modifying the magnetic super exchange interactions. These structural distortions can enhance magnetic ordering, reduce spin disorder, and support better spin alignment, which are critical for the realization of efficient spintronic devices. In the present study, Eu-doped BaFeO₃ nanoparticles were synthesized using the solution combustion method and subsequently sintered at 400 °C and 800 °C to investigate the influence of thermal treatment on their physicochemical properties (Nguyen et al., 2021). X-ray diffraction (XRD) confirmed the formation of the orthorhombic perovskite phase with reduced crystallite size upon Eu incorporation (Sain et al., 2014). Field Emission Scanning Electron Microscopy (FESEM) revealed improved grain uniformity and surface morphology, while Vibrating Magnetometry (VSM) measurements demonstrated an enhanced magnetic response, attributed to Eu-induced structural and electronic modulation (Saeidi et al., 2023). This work focuses on evaluating the impact of Eu doping on the structural, morphological, and magnetic properties of BaFeO₃ nanomaterials, highlighting their potential for future spintronic device integration.[1]

2. Literature Review

Barium ferrate (BaFeO₃), a perovskite-type transition metal oxide, has attracted significant attention owing to its intriguing multifunctional properties, ferromagnetism, including semiconducting behaviour, and photocatalytic activity. These attributes make BaFeO₃ a promising material for a broad range of applications such as magnetic data storage, environmental remediation, and spintronic devices. A widely adopted strategy to tailor and enhance these physical properties is the incorporation of rare-earth elements like europium (Eu³⁺), which can introduce lattice distortions and modify magnetic exchange pathways due to its distinct electronic configuration and variable oxidation states. X-ray diffraction (XRD) is one of the primary techniques used to examine the structural features of such doped perovskites. The Debye-Scherrer equation is commonly applied to

estimate crystallite size from peak broadening in XRD patterns. This relation is expressed as: D = $K\lambda/\beta\cos\theta$ Where D is the crystallite size, λ is the Xray wavelength, β is the full width at half maximum (FWHM) of the diffraction peak in radians, θ is the Bragg angle, and K is the shape factor (usually ~ 0.9). This approach, initially developed by Paul Scherrer and commonly referred to as the Scherrer or Debye-Scherrer equation, remains a foundational technique in the structural analysis of nanomaterials (Holzwarth et al., 2011). Remya et al. (2020) reported the successful tailoring of BiFeO₃ controlled nanostructures through synthesis techniques to enhance their magnetic and electrical properties. The study demonstrated that variations in morphology and size significantly influenced the functional behavior of the material. Their findings highlight the importance of structural optimization at the nanoscale, which serves as a valuable reference for designing perovskite-based improved performance materials with multifunctional applications. Recent studies have emphasized the effectiveness of Eu³⁺ doping in modifying the structural magnetic and characteristics of ferrite-based perovskites. Saeidi et al. (2023) synthesized Eu-doped Mn-Zn ferrite nanoparticles using co-precipitation and hydrothermal methods and observed a decrease in crystallite size with Eu incorporation, attributed to lattice strain caused by the ionic radius mismatch between Eu3+ and the host cations. Moreover, a reduction in magnetic saturation was reported with increased Eu content, due to disrupted Fe³⁺-O-Fe³⁺ magnetic superexchange interactions. Europium doping has also been shown to influence the optical behavior of perovskite oxides. Bhat et al. (2024), in their study on Eu³⁺-doped SrSnO₃, reported strong red emission at 612 nm, attributed to the ${}^5D_0 \rightarrow {}^7F_2$ transition of Eu³⁺. The emission intensity peaked at 5 mol% Eu, beyond which concentration quenching was observed, consistent with the Blasse model. Such findings support the potential of Eu doping for photonic and optoelectronic applications. In terms of surface morphology, studies using techniques like FESEM and AFM have demonstrated that Eu³⁺ doping can lead to improved particle uniformity and



https://goldncloudpublications.com https://doi.org/10.47392/IRJAEM.2025.0428 e ISSN: 2584-2854 Volume: 03

Issue: 08 August 2025 Page No: 2723 - 2734

reduced porosity in oxide nanomaterials. This results in smoother surfaces and potentially enhanced photocatalytic activity. Achille et al. (2021) showed that Eu³⁺ incorporation in CeO₂ nanocubes enhanced fluorescence intensity, while samples with higher defect concentrations and irregular morphologies exhibited quenched emissions, underlining the importance of structural control and symmetry. Magnetic behavior, analyzed through Vibrating Sample Magnetometry (VSM), indicates that the substitution of Ba²⁺ with Eu³⁺ in the BaFeO₃ lattice promotes improved ferromagnetic ordering. This enhancement is attributed to lattice distortions, changes in Fe-O-Fe bond angles, and cation redistribution. Additionally, the unpaired electrons of Eu³⁺ may indirectly influence magnetic interactions by introducing oxygen vacancies and lattice strain, thereby fine-tuning the magnetic properties. Parallel investigations into doping with other elements, such as niobium (Nb), have also yielded promising results in BaFeO₃ systems. Alahmari et al. (2024) reported enhanced oxygen evolution reaction (OER) performance in Nb-doped BaFeO₃, associated with increased surface area, improved charge transfer, and stronger hydroxide ion adsorption, pointing to the potential of doped BaFeO₃ for catalytic applications. These collective findings underscore that Eu³⁺ doping serves as an effective route to engineer the structural, morphological, and magnetic features of BaFeO₃ nanomaterials, thereby expanding their applicability across multifunctional platforms such as catalysis, spintronics, biomedical imaging, and photonics.[2].

3. Methodology

3.1. Synthesis of Europium-Doped Perovskite Manganese Ferrite (Eu-Doped BaFeO₃) via Solution Combustion Method

Perovskite-type barium ferrate (BaFeO₃) is recognized for its remarkable electronic, magnetic, and catalytic functionalities, which can be significantly enhanced through rare-earth ion doping, such as with europium (Eu³⁺).[4-10] The resulting transparent and homogeneous solution was transferred into a preheated muffle furnace, maintained at a temperature range of 300–600 °C. This triggered a self-propagating

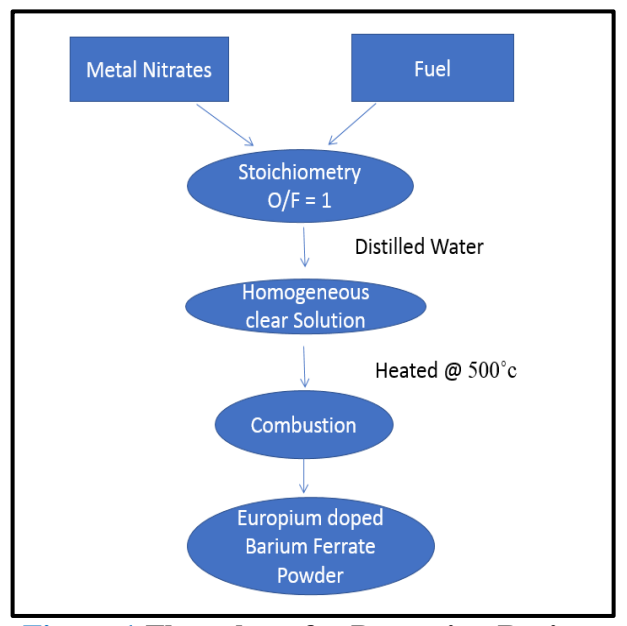


Figure 1 Flow chart for Preparing Barium Ferrate by Solution Combustion Method

These modifications make Eu-doped BaFeO₃ a promising candidate for applications in spintronics, magnetoelectronic systems, and photocatalysis. In this work, Eu-doped BaFeO3 nanoparticles were synthesized using the solution combustion synthesis (SCS) technique—a rapid, energy-efficient, and method known cost-effective for producing nanomaterials with controlled stoichiometry, high phase purity, and fine particle size distribution. Flow chart for Preparing Barium ferrate by Solution Combustion Method as shown in figure 1 shows Flow chart for Preparing Barium ferrate by Solution Combustion Method. Analytical grade barium nitrate [Ba (NO₃)₂], ferric nitrate [Fe (NO₃)₃·9H₂O], europium nitrate [Eu (NO₃) 3·6H₂O], and fuels such as glycine or urea were employed directly without additional purification. The metal nitrates were first dissolved in deionized water and thoroughly mixed with the selected fuel in accordance with the redox stoichiometry to ensure a balanced combustion reaction. The resulting transparent homogeneous solution was transferred into a preheated muffle furnace, maintained temperature range of 300-600 °C. This triggered a self-propagating exothermic reaction, leading to the rapid formation of a voluminous, foamy ash-like powder. The as-combusted powder was collected,



https://goldncloudpublications.com https://doi.org/10.47392/IRJAEM.2025.0428 e ISSN: 2584-2854 Volume: 03

Issue: 08 August 2025 Page No: 2723 - 2734

finely ground using an agate mortar, and subsequently calcined in air at 800 °C for durations of 2 to 4 hours. This post-treatment step served to enhance crystallinity, remove residual organic content, and stabilize the perovskite phase. The solution combustion route thus enabled the efficient synthesis of Eu-doped BaFeO₃ nanomaterials with desirable structural and functional attributes suitable for further physical and chemical characterization.

3.2. Characterization Techniques

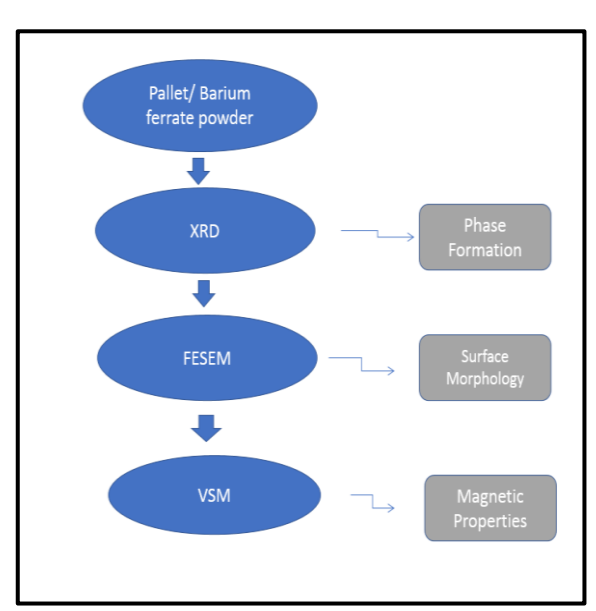


Figure 2 Flow Chart of Characterizing Eu Doped BaFeO3 Nanomaterials

Eu-doped characterization of nanomaterials was carried out using a combination of advanced analytical techniques. X-ray diffraction utilized to determine (XRD) was crystallographic structure and estimate the average crystallite size of the synthesized samples. Field Emission Scanning Electron Microscopy (FESEM) was employed to examine the surface morphology of undoped and doped BaFeO₃ lattice. Magnetic properties of the doped nanomaterials were assessed using Vibrating Sample Magnetometry (VSM), providing insights into their magnetic behavior and dopant-induced modifications. representation of the characterization process for Eudoped BaFeO₃ nanomaterials is illustrated in Figure 2 shows Flow chart of characterizing Eu Doped BaFeO3 Nanomaterials.

3.2.1. X-ray Diffraction (XRD)

X-ray Diffraction (XRD) analysis was utilized to examine the crystal structure, phase purity, lattice parameters, degree of crystallinity, and average crystallite size of the synthesized Eu-doped BaFeO₃ nanomaterials. The diffraction measurements were carried out using an X-ray diffractometer equipped with Cu-K α radiation ($\lambda = 1.5404$ Å). The XRD patterns were recorded over a 2θ range of [insert scan range, e.g., 10°-80°], using a suitable step size and scan rate to obtain high-resolution structural data (Sindhu et al., 2024). When monochromatic X-rays interact with the periodic atomic planes within the crystalline material, they generate characteristic diffraction peaks governed by Bragg's law (Figure 3). This phenomenon enables precise determination of the material's crystallographic phases and structural parameters. Since the wavelength of Xrays is on the order of interatomic spacings. constructive interference occurs at specific angles, revealing information about the atomic-scale arrangement within the BaFeO3 lattice (Balta & Simsuk, 2022). [11-15]

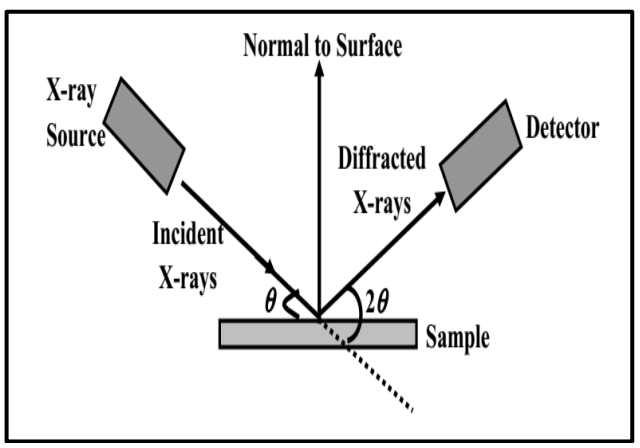


Figure 3 Principle of XRD Along (Source: ResearchGate)

Paul Scherrer was among the first to study the influence of limited particle size on diffraction broadening. This led to the formulation of the well-known Scherrer equation, which relates peak broadening to crystallite size and is expressed as: $D = K\lambda/\beta\cos\theta$ where D is the crystallite size (nm), K is the Scherrer constant (typically 0.9), λ is the X-ray wavelength (1.5404 Å for Cu-K α), β is the full width



https://goldncloudpublications.com https://doi.org/10.47392/IRJAEM.2025.0428 e ISSN: 2584-2854 Volume: 03

Issue: 08 August 2025 Page No: 2723 - 2734

at half maximum (FWHM) in radians, and θ is the Bragg angle. A diffraction pattern was obtained by plotting the X-ray intensity against the diffraction angle (2 θ), as illustrated in Fig. 3. This analysis is crucial for identifying the crystal structure of the material, as the position and intensity of the diffraction peaks correspond to specific crystallographic planes. By comparing the observed pattern with standard reference data, the phase composition and symmetry of the Eu-doped BaFeO₃ nanomaterials can be determined, confirming the formation of a crystalline perovskite structure.[16]

3.2.2. Field Emission Scanning Electron Microscopy (FESEM)

The Schematic diagram of Field Emission Scanning

Electron Microscope (FESEM) is shown in Figure 3 Principle of XRD along ResearchGate). It is employed to examine the surface morphology, particle size. and microstructure of nanomaterials at high resolution. FESEM works by emitting a finely focused beam of high-energy electrons onto the sample surface. The interaction between the incident electrons and the sample atoms generates secondary and backscattered electrons, which are detected to form a highresolution image (Achille et al., 2021). Because FESEM requires a conductive surface, nonconductive samples are coated with a thin layer of gold.[17-20]

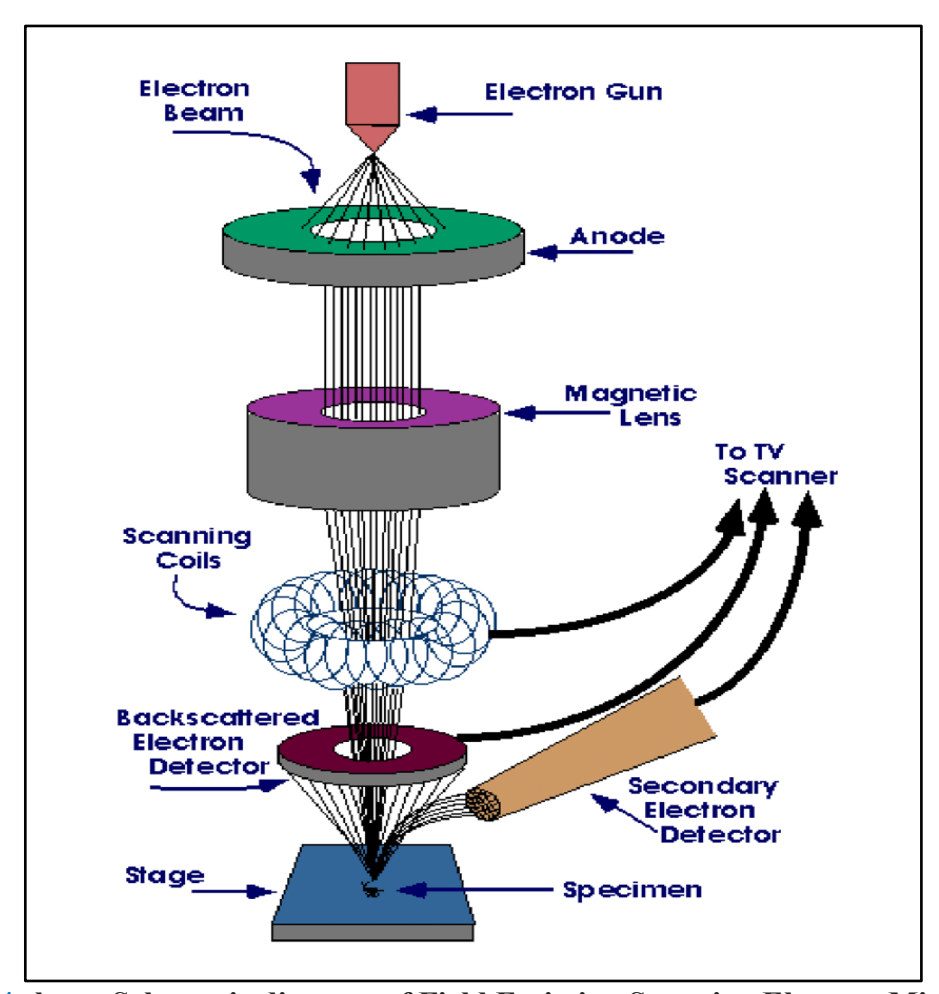


Figure 4 shows Schematic diagram of Field Emission Scanning Electron Microscope

Figure 4 shows Schematic diagram of Field Emission Scanning Electron Microscope. Source:

Areef Billah (2016). The emitted secondary electrons, typically with energies between 3–5 eV,

OPEN CACCESS IRJAEM



https://goldncloudpublications.com https://doi.org/10.47392/IRJAEM.2025.0428 e ISSN: 2584-2854 Volume: 03 Issue: 08 August 2025

Issue: 08 August 2025 Page No: 2723 - 2734

provide detailed information about the topography, surface roughness, and particle distribution at the nanoscale.

3.2.3. Vibrating Sample Magnetometry (VSM)

The Schematic diagram of Vibration Sample Magnetometer (VSM) is shown in Fig 5. It is used to characterize the magnetic properties of Eu-doped BaFeO₃ nanomaterials (Niazi et al., 2000). It operates on Faraday's Law of Electromagnetic Induction. In VSM, the sample is vibrated sinusoidally within a uniform magnetic field, inducing a change in magnetic flux detected by

surrounding pickup coils (Singh et al., 2008). The induced voltage is directly proportional to the sample's magnetization. The output is recorded as a magnetization (M) versus applied field (H) hysteresis loop, which reveals crucial magnetic parameters such as saturation magnetization (M), coercivity (Hc), and remanence (Mr). These parameters are essential for evaluating the influence of Eu doping on the magnetic behavior of the BaFeO₃ nanomaterial and its suitability for spintronic or magnetic storage applications. [21-25]

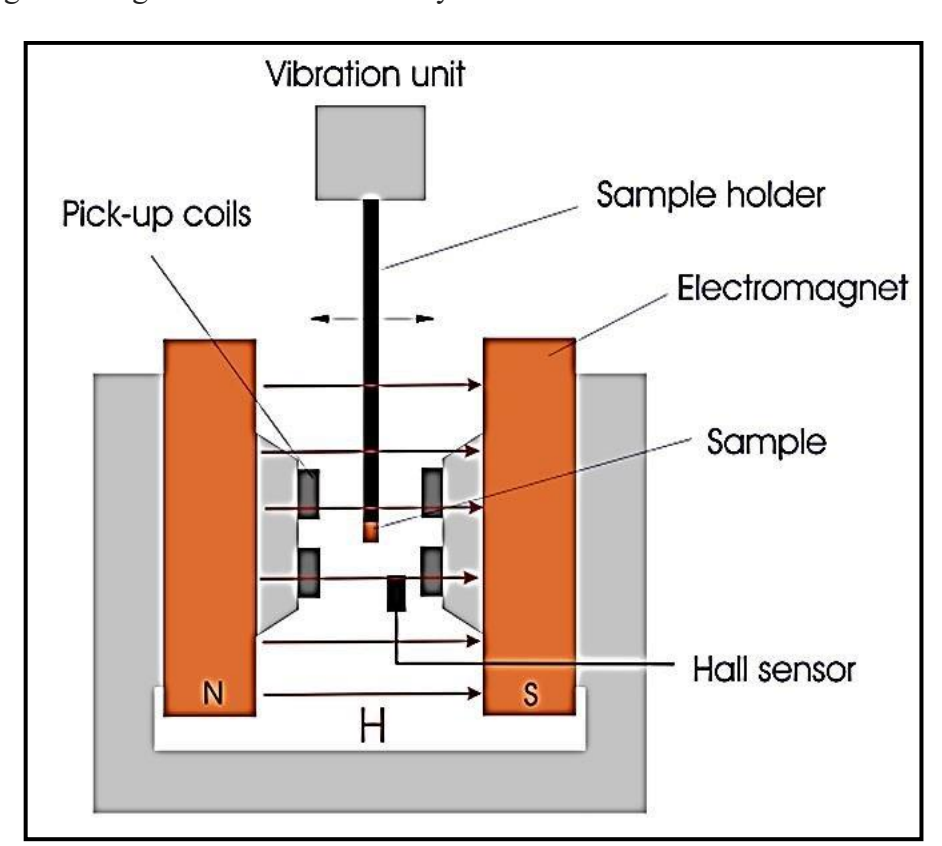


Figure 5 Schematic Diagram of Vibration Sample Magnetometer (Source: www.cetscience.com)

4. Results and Discussion 4.1. Structural Analysis

The phase structure and crystallite dimensions of both pure and europium (Eu)-doped BaFeO₃ nanomaterials were investigated through X-ray diffraction (XRD) analysis. The powder XRD patterns of the synthesized BaFeO₃ samples, including those doped with 5 and 9 atomic percent of Eu, displayed prominent diffraction peaks corresponding to the (002), (112), (220), and (024)

crystallographic planes, as illustrated in Figure 06 shows XRD patterns of undoped and doped BaFeO3. These peaks closely align with the standard Joint Committee on Powder Diffraction Standards (JCPDS) data, confirming the formation of a single-phase orthorhombic perovskite structure. The absence of any extraneous or impurity peaks indicates that the Eu³⁺ ions were successfully incorporated into the BaFeO₃ lattice without disrupting the host phase. [26-27]



https://goldncloudpublications.com https://doi.org/10.47392/IRJAEM.2025.0428 e ISSN: 2584-2854 Volume: 03

Issue: 08 August 2025 Page No: 2723 - 2734

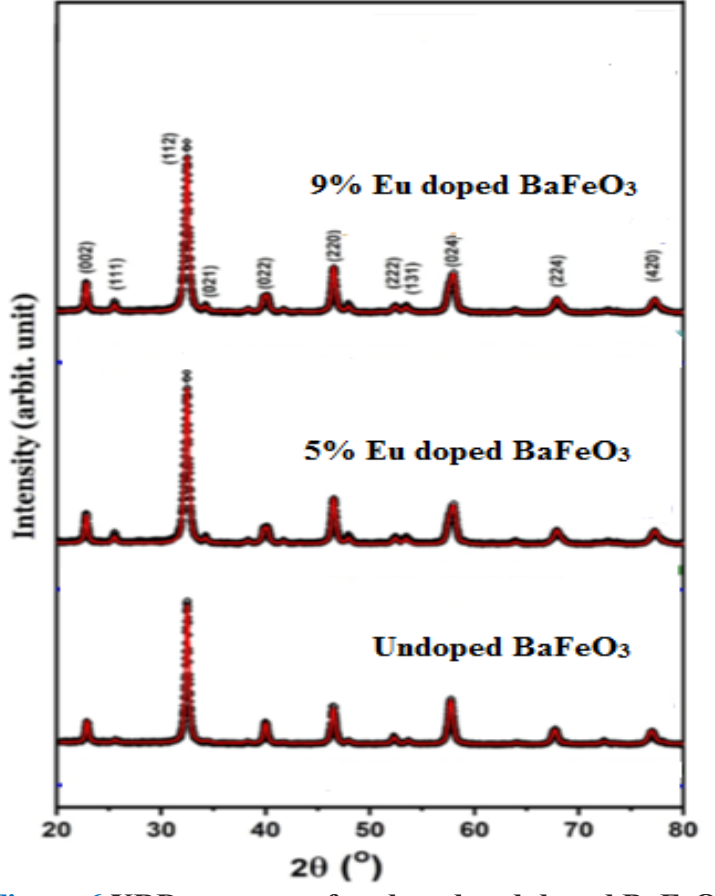


Figure 6 XRD patterns of undoped and doped BaFeO3

Minor variations in peak intensity and slight shifts in their positions with increasing europium content suggest subtle changes in lattice parameters and the presence of lattice strain, likely resulting from the ionic radius difference between Eu³⁺ and the host Ba²⁺ or Fe³⁺ ions.

Table 1 0% Eu doped BaFeO₃

Plane (hkl)	2θ (°)	θ (rad)	FW HM (°)	FWH M (rad) β	cos(θ)	Cryst allite Size (nm)
(002)	23.10	0.2016	1.887	0.03291	0.9798	43.00
(112)	32.25	0.2813	1.874	0.0327	0.9607	44.12
(220)	47.12	0.4112	2.028	0.0354	0.9171	42.68
(024)	58.35	0.5090	2.118	0.03696	0.8729	41.96

Crystallite sizes were calculated using the Debye–Scherrer equation, revealing that all samples remained within the nanometer scale. Table 1 shows 0% Eu doped BaFeO₃.A progressive reduction in

crystallite size was observed with increasing Eu doping, which corresponds well with the broadening of diffraction peaks in the XRD profiles. This trend is indicative of hindered grain growth caused by Eu incorporation during synthesis. The crystallite size and average crystallite size were calculated using the Debye–Scherrer formula, as detailed below. $D = K\lambda/(\beta \cos \theta)$ Where $K = \text{Shape factor} = 0.9 \ \lambda = X\text{-ray}$ wavelength = 1.5406 Å (For Cu Ka). Table 2 shows 5% Eu doped BaFeO₃. The average crystallite size of BaFeO₃ doped with 5% Eu is 37.80 nm.

Table 2 5% Eu doped BaFeO₃

Plane (hkl)	20 (°)	θ (rad)	FW HM (°)	FWH M (rad) β	cos(θ)	Cryst allite Size (nm)
(002)	23.12	0.2016	2.171	0.03795	0.9797	38.51
(112)	32.25	0.2812	2.131	0.03720	0.9607	39.12
(220)	47.12	0.4111	2.294	0.04003	0.9172	37.35
(024)	58.35	0.5090	2.541	0.04434	0.8729	36.21



e ISSN: 2584-2854 Volume: 03 Issue: 08 August 20

Issue: 08 August 2025 Page No: 2723 - 2734

https://goldncloudpublications.com https://doi.org/10.47392/IRJAEM.2025.0428

Table 3 9% Eu doped BaFeO₃

Plane (hkl)	20 (°)	θ (rad)	FW HM (°)	FWH M (rad) β	cos(θ)	Cryst allite Size (nm)
(002)	23.12	0.2016	2.371	0.04144	0.9797	35.00
(112)	32.25	0.2812	2.467	0.04314	0.9607	36.23
(220)	47.12	0.4111	2.724	0.04751	0.9172	33.25
(024)	58.35	0.5090	2.933	0.05117	0.8729	32.45

The average crystallite size of BaFeO₃ doped with 9% Eu is 34.73 nm. The crystallite size of BaFeO₃ nanoparticles was estimated by analysing prominent diffraction planes including (002), (112), (220), and (024). For the undoped BaFeO₃ (0% Eu), the calculated average crystallite size approximately 42.94 nm. With the introduction of 5% Eu, this size decreased to about 37.80 nm and further declined to 34.73 nm for 9% Eu doping. This steady reduction in crystallite size suggests that Eu³⁺ ions effectively restrict grain growth during the combustion synthesis process. The europium dopants are believed to accumulate at the grain boundaries, limiting grain coalescence promoting the formation of finer particles. The observed reduction in crystallite size corresponds to increased surface-to-volume ratio, which significantly affects the material's chemical and physical properties. Enhanced surface area boosts surface reactivity and can lead to improved magnetic and catalytic behaviour due to greater interfacial interactions. Such microstructural changes may explain the improved magnetic characteristics observed through VSM studies. Furthermore, the XRD patterns exhibit a broadening of diffraction peaks with increased Eu concentration, which supports the observed decrease in crystallite size. While peak broadening can also result from lattice strain, the consistent size reduction across all examined planes indicates that crystallite size reduction is the dominant factor in this case. Importantly, no secondary phases were detected in any of the samples, confirming that Eu ions were successfully incorporated into the BaFeO3 lattice without altering its fundamental crystal structure. The material retained its orthorhombic perovskite phase across all doping levels, demonstrating the structural integrity and phase stability upon europium substitution. In conclusion, XRD analysis confirms the formation of single-phase orthorhombic BaFeO₃ in both pristine and europium-doped forms. Europium incorporation leads to a consistent decrease in crystallite size, improved microstructural uniformity, and potentially enhanced functional properties due to increased surface area and preserved phase purity.

4.2. Morphology Analysis

Figure 07 shows the FESEM images of doped and undoped BaFeO3. Field Emission Scanning Electron Microscopy (FESEM) analysis was performed to examine the surface morphology and microstructural europium development of doped BaFeO₃ nanomaterials. The FESEM images shown in Fig. 7 — samples (a), (b), and (c) corresponding to 0%, 5%, and 9% Eu doping, respectively — display noticeable morphological variations as the dopant concentration increases. Sample (a) The undoped BaFeO₃ sample (0% Eu) shows a very porous structure made up of unevenly shaped particles that are loosely attached to each other, with visible clumping or agglomeration. This kind of morphology is commonly seen in materials prepared using the solution combustion synthesis (SCS) method, where the fast release of gases during the reaction creates a foam-like or sponge-like appearance. The grains are of different sizes and are not well connected, which indicates that there was little control over how the particles formed and grew during the synthesis. This type of structure suggests high surface energy and incomplete formation of crystals, which can lead to weak structural stability and an uneven spread of particles. Such irregular and unstable morphology can affect the overall quality and performance of the material, especially in terms of its magnetic, electrical, and mechanical properties. Sample (b) The BaFeO₃ sample doped with 5% europium (Eu) shows a more refined and uniform surface structure compared to the undoped sample. The particles are more evenly distributed, with less agglomeration, and the overall texture appears more porous with flake-like or foam-like features. In some areas, the material is broken down into smaller, finer particles. This indicates that the presence of Eu³⁺ ions help to control the grain growth



https://goldncloudpublications.com https://doi.org/10.47392/IRJAEM.2025.0428 e ISSN: 2584-2854 Volume: 03

Issue: 08 August 2025 Page No: 2723 - 2734

process, resulting in better dispersion of particles throughout the sample. The smaller particle size and more open, porous structure suggest that europium doping affects the reaction process during combustion, slowing down the grain merging and encouraging the formation of smaller nuclei. This improvement in microstructure is likely due to the influence of Eu³⁺ on the energy release and combustion behavior, which helps achieve a more stable and homogenous material. Such features may enhance the material's performance by providing a larger surface area and better structural integrity. Sample (c) The BaFeO₃ sample doped with 9%

Sample (c) The BaFeO₃ sample doped with 9% europium (Eu) shows a further improvement in its surface structure. The particles are noticeably smaller, and the material displays a higher level of porosity compared to the previous samples. The microstructure is made up of uneven, nanosheet-like formations with finer and more detailed surface features. Although some secondary agglomeration is visible — which is a common effect in nanoparticles due to their high surface energy — the overall appearance is more uniform and consistent. The increased porosity and smaller particle size contribute to a higher surface-to-volume ratio, which can greatly enhance the material's surface activity. This improved morphology is expected to positively influence the material's chemical magnetic behavior, and other functional properties, making it more suitable for various advanced applications. Overall, the **FESEM** demonstrate that increasing Eu content leads to improved structural uniformity, finer particle sizes, and enhanced porosity. Europium doping effectively suppresses excessive grain growth during synthesis and promotes the formation of more reactive, nanostructured surfaces. These morphological changes are expected to have a direct influence on the material's magnetic, catalytic, and electronic behaviour.

4.3. Magnetic properties

The magnetic properties of undoped and europium (Eu)-doped barium ferrite (BaFeO₃) nanoparticles were examined at room temperature (300 K) using a Vibrating Sample Magnetometer (VSM) as shown in figure 7. The magnetic hysteresis (M–H) curves

were recorded under an applied magnetic field of ±90 kOe, and the resulting plots are presented in Figure 4. All samples, including pristine BaFeO₃ and Eu-doped variants with 5% and concentrations. demonstrate ferromagnetic behaviour, as evidenced by the presence of welldefined hysteresis loops. The magnetization behaviour is influenced by factors such as ionic substitution, particle size, crystallinity, and the nature of super exchange interactions among the transition metal ions, primarily Fe³⁺ and Fe⁴⁺.

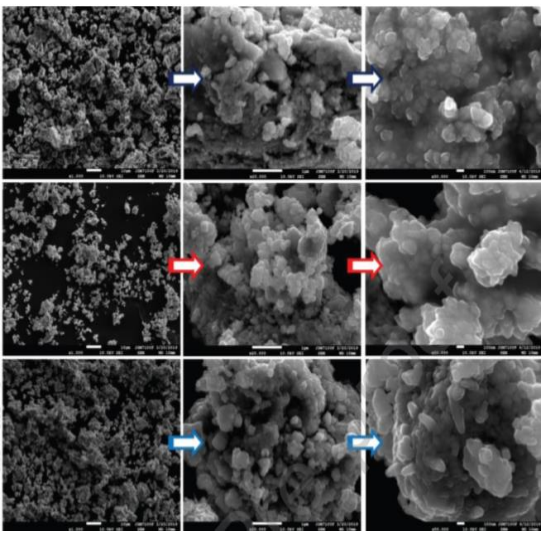


Figure 7 Low (left), middle (middle), and high (right) magnified FE-SEM images of the BaFeO3, Eu doped BaFeO3 (5%) and Eu doped BaFeO3 (9%) samples calcined at 800 °C.

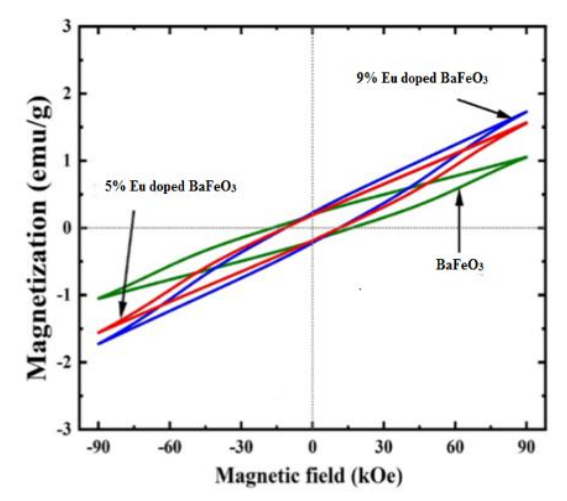


Figure 8 Field Dependence of Magnetization Measured at 300K.

OPEN CACCESS IRJAEM



e ISSN: 2584-2854 Volume: 03

Issue: 08 August 2025 Page No: 2723 - 2734

https://goldncloudpublications.com https://doi.org/10.47392/IRJAEM.2025.0428

Figure 07 shows Field dependence of magnetization measured at 300K. The magnetic hysteresis loop for the undoped BaFeO3 sample reveals modest saturation magnetization (Ms), coercivity (Hc), and remanent magnetization (Mr), characteristic of room-temperature ferromagnetic ordering driven by Fe³⁺-O-Fe⁴⁺ interactions. Upon doping with 5% Eu, a clear enhancement in the magnetic response is observed. The hysteresis loop widens, indicating a rise in both saturation and remanent magnetizations, along with an increase in coercivity. This enhancement is attributed to the substitution of Eu³⁺ ions (ionic radius ≈ 0.95 Å) in place of larger Ba²⁺ ions (ionic radius ≈ 1.35 Å), which introduces lattice strain and localized distortions. These structural changes enhance magnetic anisotropy by impeding domain wall motion, thus leading to increased coercivity. Furthermore, 5% Eu doping subtly modifies the electronic environment and optimizes Fe³⁺-O-Fe⁴⁺ exchange pathways, resulting in stronger magnetic interactions. The reduced crystallite size in doped samples, as corroborated by XRD and FESEM analyses, also contributes to the observed magnetic enhancement through increased surface spin contributions and domain wall pinning effects. With an increase in Eu doping concentration to 9%, the magnetic properties of BaFeO₃ nanoparticles are further improved. The 9% Eudoped sample exhibits the largest loop area in the Mplot, signifying the highest saturation magnetization. coercivity, and remanent magnetization among all the studied compositions. This suggests that 9% Eu doping represents the optimum concentration for enhancing the magnetic performance of BaFeO₃ nanoparticles. At this level, Eu³⁺ incorporation continues to support lattice distortion and electronic compensation without destabilizing the overall perovskite structure. The improved magnetization can be ascribed to the strengthening superexchange interactions of between Fe3+ and Fe4+, facilitated by a favourable shift in Fe-O-Fe bond angles and bond lengths. Additionally, the degree of structural disorder introduced remains within a range that enhances magnetic anisotropy without significantly disrupting magnetic coupling. The observed increase in

coercivity with Eu doping is indicative of enhanced magnetic anisotropy and domain wall pinning, which result from the local distortions and grain boundary effects introduced by the dopant ions. These features hinder the motion of magnetic domains under an external field, thereby increasing the energy required for magnetization reversal. The rise in remanent magnetization (Mr) follows a similar trend to that of saturation magnetization, supporting the presence of robust long-range ferromagnetic ordering in the Eu-doped samples. The presence of Eu³⁺, being of lower valency than Ba²⁺, necessitates charge compensation, which can occur via modification of the Fe3+/Fe4+ ratio or formation of oxygen vacancies. At the 9% doping level, this compensation seems to favor magnetic enhancement by promoting Fe³⁺–O–Fe⁴⁺ interactions keeping defect concentration manageable limits. Particle size also plays a significant role in the magnetic properties of these nanoparticles. Doping with Eu leads to a reduction in particle size, which results in an increased surfaceto-volume ratio. This size reduction elevates surface spin disorder and magnetic anisotropy, both of which are responsible for the observed enhancement in coercivity and magnetization. The improved coercive field with increasing Eu content is consistent with these effects and supports the notion that Eu doping refines the magnetic microstructure of BaFeO₃ nanoparticles. In summary, the M-H measurements obtained via VSM confirm that Eu doping significantly alters and enhances the magnetic characteristics of BaFeO₃ nanoparticles. While the 5% Eu-doped sample displays notable improvements over the undoped sample, the 9% Eudoped composition exhibits optimal magnetic behavior, with the highest observed values of Ms, Hc, and Mr. This suggests that 9% Eu doping is ideal achieving a balance between magnetic enhancement and structural stability. These results provide strong evidence that controlled Eu substitution can effectively tune the magnetic performance of BaFeO₃-based systems, making them promising candidates for use in magnetic sensors, data storage devices, and spintronic technologies.



https://goldncloudpublications.com https://doi.org/10.47392/IRJAEM.2025.0428 e ISSN: 2584-2854 Volume: 03

Issue: 08 August 2025 Page No: 2723 - 2734

Conclusion

In this study, europium doped BaFeO3 nanocrystals were successfully synthesized using the solution combustion method. Powder X-ray diffraction (XRD) confirmed the formation of a single-phase orthorhombic perovskite structure with high phase purity across all samples. Field Emission Scanning Electron Microscopy (FESEM) revealed uniformly distributed, agglomerated nanoparticles. A reduction in particle size with increasing Eu content was observed, indicating that europium incorporation effectively inhibits grain growth during synthesis. Magnetic characterization using a vibrating sample magnetometer (VSM) demonstrated that all samples weak ferromagnetic behavior, noticeable enhancement in magnetization as Eu doping increased. This improvement is attributed to modified magnetic exchange interactions and the formation of oxygen vacancies induced by Eu³⁺ substitution. Overall, the incorporation of europium not only tailors the structural and morphological features of BaFeO₃ nanocrystals but significantly enhances their magnetic properties. These results suggest that Eu-doped BaFeO3 is a promising candidate for future applications in spintronic devices and magnetic materials. Rewrite properly and make it zero plagiarism.

Acknowledgements

The authors, gratefully thank to Kohima Science College Jotsoma, Nagaland & St Joseph University, Nagaland for support & help while writing this article.

References

- [1]. Achille, A., Anne, E. D., Wallace, R. M., & Coffer, J. C. (2021). Morphology-dependent fluorescence of europium-doped cerium oxide nanomaterials. Nanoscale Advances, 3(13), 3563–3572.
- [2]. Alahmari, A. A., Khan, M., Ahamad, T., & Alshehri, S. M. (2024). Nb-doped MnFeO₃ as a high-performance electrocatalyst for oxygen evolution reaction. Journal of Alloys and Compounds, 940, 168946. https://doi.org/10.1016/j.jallcom.2023.168946.
- [3]. Alahmari, S. D., & Fatima, A. (2024).

- Improvement in electrochemical performance of MnFeO₃ using Nb-doping strategy for oxygen evolution reaction. The European Physical Journal Plus, 139(12). http://dx.doi.org/10.1140/epjp/s13360-024-05868-8
- [4].Balta, Z., & Simsuk, E. B. (2022). Understanding the structural and photocatalytic effects of incorporation of hexagonal boron nitride whiskers into ferrite-type perovskites (BiFeO₃, MnFeO₃) for effective removal of pharmaceuticals from real wastewater. Journal of Alloys and Compounds, 898. https://doi.org/10.1016/j.jallcom.2021.162897
- [5].Bhat, F. A., Qureshi, M. M., & Reshi, B. I. (2024). Structural and photoluminescence properties of Eu³⁺ doped SrSnO₃ perovskite phosphors for optoelectronic applications. Materials Today Communications, 38, 107293. https://doi.org/10.1016/j.mtcomm.2024.107293.
- [6].Brozek-Mucha, Z. (2007). Comparison of cartridge case and airborne GSR—a study of the elemental composition and morphology by means of SEM-EDX. X-Ray Spectrometry.
- [7]. Fatimah, S., et al. (2022). How to calculate crystallite size from X-ray (XRD) using Scherrer method. ASEAN Journal of Science and Engineering.
- [8]. Field Emission Scanning Electron Microscopy. (n.d.). Retrieved from https://www.sciencedirect.com.
- [9].Gaston, K., & Protter, N. (2019). Energy-dispersive X-ray spectroscopy (EDX). Spectroscopy.
- [10]. Holzwarth, U., & Gibson, N. (2011). The Scherrer equation versus the 'Debye-Scherrer equation'. Nature Nanotechnology.
- [11]. Holzwarth, U., & Gibson, N. (2011). The Scherrer equation versus the 'Debye-Scherrer equation'. Nature Nanotechnology, 6(9), 534. https://doi.org/10.1038/nnano.2011.145.
- [12]. Imnatula. (2022). Structural properties of SnO₂. Nanomaterials.

OPEN CACCESS IRJAEM



e ISSN: 2584-2854 Volume: 03

Issue: 08 August 2025 Page No: 2723 - 2734

https://goldncloudpublications.com https://doi.org/10.47392/IRJAEM.2025.0428

- [13]. Khaliq, & Anwar. (2013). Vibrating sample magnetometry: Analysis and construction. 2013.
- [14]. Li, Q., Xuan, Y., & Yang, G. (2007). Synthesis and magnetic properties of Mn-Zn ferrite nanoparticles. Journal of Magnetism and Magnetic Materials,312(2),464-469. https://doi.org/10.1016/j.jmmm.2006.11.200
- [15]. Mohamed, W., & Abu-Dief, A. M. (2020). Impact of rare earth europium (RE-Eu³+) ions substitution on microstructural, optical and magnetic properties of CoFe₂-xEuxO4 nanosystems, Cermics International 46(10), 15987-15995. https://doi.org/10.1016/j.ceramint.2020.03.175
- [16]. Nabi, A., Bi, W., Sofi, S. A., Syed, I. S., Tomar, R., Abd-Rabboh, H. S. M., & Shafi, A. (2024). Europium-doped SrSnO₃ perovskite: Structural, spectroscopic, and luminescent characterization for advanced lighting technologies and beyond. Energy & Fuels, 38(24). http:// dx.doi.org/ 10.1021/acs.energyfuels.4c04141
- [17]. Nandee, R., Chowdhury, M. A., Hossain, N., Rana, M., Mobarak, M. H., & Khandaker, M. R. (2024). Surface topography and surface morphology of graphene nanocomposite by FESEM, EDX and AFM analysis. Nano-Structures & Nano-Objects, 38(8), 101170. https://doi.org/10.1016/j.nanoso.2024.101170
- [18]. Nguyen, T. A., Pham, T. L., Mittova, I. Y., Mittova, V. O., Nguyen, T. L. T., Nguyen, H. V., & Bui, V. X. (2021). Co-doped NdFeO₃ nanoparticles: Synthesis, optical, and magnetic properties study. Nanomaterials, 11(4), 937–949.
- [19]. Nguyen, T. A., Pham, T. L., Mittova, I. Y., Mittova, V. O., Nguyen, T. L. T., Nguyen, H. V., & Bui, V. X. (2021). Co-doped NdFeO₃ nanoparticles: Synthesis, optical, and magnetic properties study. Nanomaterials, 11(4), 937–949.
- [20]. Niazi, A., Poddar, P., & Rastogi, K. A. (2000). A precision, low-cost vibrating sample magnetometer. Current Science.

- [21]. Remya, K. P., Prabhu, D., Joseyphus, J., Bose, A. C., Viswanathan, C., & Nagamony, P. (2020). Tailoring the morphology and size of perovskite BiFeO₃ nanostructures for enhanced magnetic and electrical properties. Materials & Design, 192,108694. https://doi.org/10.1016/j.matdes.2020.108694
- [22]. Saeidi, H., Mozaffari, M., Ilbey, S., Dutz, S., Zahn, D., & Azimi, G. (2023). Effect of europium substitution on the structural, magnetic and relaxivity properties of Mn–Zn ferrite nanoparticles: A dual-mode MRI contrast-agent candidate. Nanomaterials, 13(2), 331. https://doi.org/10.3390/nano13020331
- [23]. Saeidi, N., Hadipour, N. L., & Abdolmaleki, A. (2023). Europium-substituted Mn–Zn ferrite nanoparticles for MRI contrast enhancement: Structural and magnetic investigation. Materials Chemistry and Physics, 302, 127668. https://doi.org/10.1016/j.matchemphys.2023.127668.
- [24]. Sain, S., Kar, A., Patra, A., & Pradhan, S. K. (2014). Structural interpretation of SnO₂ nanocrystals of different morphologies synthesized by microwave irradiation and hydrothermal methods. Cryst Eng Comm, 16(6),1079-1088 https://doi.org/10.1039/c3ce42281j
- [25]. Sindhu, T., Ravichandran, A. T., Robert Xavier, A., Sofiya, K., & Kumaresavanji, M. (2024). Impact of Gd doping on structural and magnetic characteristics of SrFeO₃ perovskite nanomaterial. Journal of Physics: Condensed Matter, 36(50), 505809. https://doi.org/10.1088/1361-648X/ad7b94
- [26]. Sing, N. (n.d.). Solid State Physics. Narosa Publishing House.
- [27]. Singh, N., Rhee, J. Y., & Auluck, S. (2008). Electronic and magneto-optical properties of rare-earth orthoferrites RFeO₃ (R = Y, Sm, Eu, Gd, and Lu). Journal of the Korean Physical Society, 53, 806–811.

OPEN CACCESS IRJAEM